Journal Pre-proofs

Mild exogenous inflammation blunts neural signatures of bounded evidence accumulation and reward prediction error processing in healthy male participants

Filippo Queirazza, Jonathan Cavanagh, Marios G. Philiastides, Rajeev Krishnadas

PII: S0889-1591(24)00325-8
DOI: https://doi.org/10.1016/j.bbi.2024.03.044
Reference: YBRBI 5445

To appear in: *Brain, Behavior, and Immunity*

Received Date: 17 October 2023
Revised Date: 21 March 2024
Accepted Date: 28 March 2024

Please cite this article as: Queirazza, F., Cavanagh, J., Philiastides, M.G., Krishnadas, R., Mild exogenous inflammation blunts neural signatures of bounded evidence accumulation and reward prediction error processing in healthy male participants, *Brain, Behavior, and Immunity* (2024), doi: https://doi.org/10.1016/j.bbi.2024.03.044

Mild exogenous inflammation blunts neural signatures of bounded evidence accumulation and reward prediction error processing in healthy male participants.

Authors:

Filippo Queirazza[1,3,*], Jonathan Cavanagh[2], Marios G. Philiastides[3^] and Rajeev Krishnadas[3,4^]

^co-senior authors

Affiliations:

[1]School of Health and Wellbeing, University of Glasgow, Glasgow, G12 0XH, UK

[2]School of Infection, Immunity and Inflammation, University of Glasgow, Glasgow, G12 8TA, UK

[3]School of Psychology and Neuroscience, University of Glasgow, Glasgow, G12 8AD, UK

[4]Department of Psychiatry, University of Cambridge, Cambridge, Cambridge Biomedical Campus, Cambridge, CB2 0AH

***Correspondence:**

Filippo.Queirazza@glasgow.ac.uk

Number of pages: 49

Number of figures: 6

Number of words (Abstract): 289

Abstract

Background: Altered neural haemodynamic activity during decision making and learning has been linked to the effects of inflammation on mood and motivated behaviours. So far, it has been reported that blunted mesolimbic dopamine reward signals are associated with inflammation-induced anhedonia and apathy. Nonetheless, it is still unclear whether inflammation impacts neural activity underpinning decision dynamics. The process of decision making involves integration of noisy evidence from the environment until a critical threshold of evidence is reached. There is growing empirical evidence that such process, which is usually referred to as bounded accumulation of decision evidence, is affected in the context of mental illness.

Methods: In a randomised, placebo-controlled, crossover study, 19 healthy male participants were allocated to placebo and typhoid vaccination. Three to four hours post-injection, participants performed a probabilistic reversal-learning task during functional magnetic resonance imaging. To capture the hidden neurocognitive operations underpinning decision-making, we devised a hybrid sequential sampling and reinforcement learning computational model. We conducted whole brain analyses informed by the modelling results to investigate the effects of inflammation on the efficiency of decision dynamics and reward learning.

Results: We found that during the decision phase of the task, typhoid vaccination attenuated neural signatures of bounded evidence accumulation in the dorsomedial prefrontal cortex, only for decisions requiring short integration time. Consistent with prior work, we showed that, in the outcome phase, mild acute inflammation blunted the reward prediction error in the bilateral ventral striatum and amygdala.

Conclusions: Our study extends current insights into the effects of inflammation on the neural mechanisms of decision making and shows that exogenous inflammation alters neural activity indexing efficiency of evidence integration, as a function of choice discriminability. Moreover, we replicate previous findings that inflammation blunts striatal reward prediction error signals.

1. Introduction

There is now compelling experimental evidence linking systemic inflammation to depression and several other psychiatric disorders (Michopoulos, Powers, Gillespie, Ressler, & Jovanovic, 2017; Miller, 2020). One of the several converging lines of evidence supporting this contention (Krishnadas & Cavanagh, 2012) has been the observation that the behavioural changes induced by acute inflammation (also known as the sickness behaviour (Dantzer & Kelley, 2007)) are the expression of an altered motivational state. While in the short-term diminished motivation is adaptive and promotes recovery, in the long run (as in chronic inflammation) it can lead to the core functional impairments commonly observed in depression (and other mental disorders) such as apathy and anhedonia (Dantzer, O'Connor, Freund, Johnson, & Kelley, 2008). Crucially, impaired motivated behaviour has been framed in terms of aberrant effort-based decision making (Husain & Roiser, 2018; Treadway, Bossaller, Shelton, & Zald, 2012).

Mesolimbic (and mesocortical) dopamine pathways play a key role in the neurobiology of motivated behaviour (Salamone, Correa, Ferrigno, et al., 2018; Salamone, Correa, Yang, Rotolo, & Presby, 2018) and proinflammatory cytokines such as interleukin-6 (IL-6) are known to disrupt monoamine metabolism, including the synthesis, release and reuptake of dopamine (Miller, Maletic, & Raison, 2009; Miller & Raison, 2016). Furthermore, at the neurocircuitry level, previous task-based neuroimaging studies have shown that exogenous inflammation attenuates haemodynamic responses to reward anticipation (Eisenberger et al., 2010; Moieni et al., 2019) or feedback (Capuron et al., 2012) in the dopamine rich ventral striatum. Consistent with these findings, elevated endogenous inflammation was associated with blunted striatal reward signals in medicated depressed patients (Burrows et al., 2021) and decreased resting state corticostriatal functional connectivity in unmedicated depressed subjects (Felger et al., 2016). These alterations in the reward circuitry have been associated with anhedonia and psychomotor slowing (Capuron et al., 2012; Felger et al., 2016) and are mediated via deficits in striatal dopamine signalling (Capuron et al., 2012).

The field of reinforcement learning (RL) (that is, learning from feedback information) has significantly contributed to bridging the explanatory gap between molecular and neuroimaging findings in inflammation research. Notably, so far neuroimaging studies have primarily focused on the reward prediction error (RPE), a mesolimbic dopaminergic teaching signal driving associative learning and motivated behaviours (Schultz, Dayan, & Montague, 1997). Considering the key role of dopamine in the context of reward learning and effort expenditure (Salamone, Correa, Ferrigno, et al., 2018; Salamone, Correa, Yang, et al., 2018; Treadway, Cooper, & Miller, 2019) aberrant RPE signalling provides a parsimonious mechanistic account of the motivational disturbances induced by acute inflammation (Dantzer et al., 2008). In support of this notion, Harrison et al. conducted a functional resonance imaging (fMRI) experiment and found that, in a sample of healthy male participants, typhoid vaccination diminished RPE activity in the ventral striatum (Harrison et al., 2016). A subsequent study extended this finding by showing that raised pro-inflammatory cytokines plasma levels induced by an acute stress paradigm were associated with reduced striatal RPE activations in a sample of healthy female subjects (Treadway et al., 2017).

While these studies have exclusively modelled neural activity associated with feedback, they have not investigated the effects of inflammation on decision dynamics at the time of choice. Bounded accumulation of noisy evidence in favour of one of two decision alternatives is a well validated domain-general theoretical account of how information is processed before committing to a response option and the rate at which decision evidence is accrued scales with choice discriminability (that is, faster for easier or more discriminable decisions and slower for more difficult or less discriminable decisions) (Ratcliff & McKoon, 2008). More generally, the computational framework of sequential sampling models (SSM) has proven an invaluable tool for dissecting distinct latent neurocognitive components underpinning continuous integration of decision evidence (Bogacz, 2007; Forstmann, Ratcliff, & Wagenmakers, 2016; Krajbich, Armel, & Rangel, 2010; Shadlen & Kiani, 2013; Verdonck, Loossens, & Philiastides, 2021) and their neural substrates (Balsdon, Verdonck, Loossens, & Philiastides, 2023; Franzen, Delis, De Sousa, Kayser, & Philiastides, 2020; Gherman & Philiastides, 2015; Kelly & O'Connell, 2013). Further developments in computational modelling have combined SSM and RL algorithms to better account for the within- and across-trial complexities of choice behaviour (Luzardo, Alonso, & Mondragon, 2017; Pedersen, Frank, & Biele, 2017). Importantly, the neural basis of evidence accumulation processes has now been also elucidated in the context of value-based decisions (Arabadzhiyska et al., 2022; Pisauro, Fouragnan, Retzler, & Philiastides, 2017).

In this study we set out to address this knowledge gap and devised a hybrid RL and SSM computational model to identify fMRI activity that supports accumulation of decision evidence and reward learning during a probabilistic reversal learning task (PRL), akin to a two-alternative forced-choice task under time pressure. Based on the proposal that the motivational changes observed in the context of acute inflammation represent an evolutionary adaptive response promoting host survival via reallocation of metabolic resources to more pressing needs such as wound healing and pathogen avoidance (Dantzer, 2001; Hart, 1988; Miller & Raison, 2016), we hypothesised that acute inflammation would be associated with differential engagement of neuronal resources required for integration of decision evidence at the time of choice as a function of perceived decision discriminability. More specifically, we predicted that, in the service of preservation of neuronal resources, inflammation would re-prioritise neuronal recruitment underpinning evidence accumulation away from decisions that are subjectively perceived as more discriminable (and thus less “worthy” of neural expenditure) towards less discriminable (and thus more “worthy” of neural expenditure) decisions.

To test this prediction, we conducted a randomised placebo-controlled cross-over trial on a sample of healthy male subjects and employed typhoid vaccination to induce a mild inflammatory response. We evaluated between-condition (that is, typhoid vaccination versus placebo) differences in haemodynamic activity representing short versus long duration of decision evidence integration (as an index of perceived decision discriminability) at the time of choice and the RPE at the time of outcome. Crucially, we found that typhoid vaccination induced a mild inflammatory response reminiscent of that observed in depression and interfered with the efficiency of the process of evidence accumulation, specifically on decisions requiring short integration times. In addition, we further validated that RPE signalling at the time of outcome was attenuated in several limbic areas of the brain, consistent with prior work (Harrison et al., 2016; Treadway et al., 2017). Our findings

extend current insights into the effects of inflammation on the neural mechanisms of decision making and the potential cognitive pathways linking inflammation to psychopathology.

2. Methods

2.1 Participants

We recruited potential participants from the School of Psychology and Neuroscience subjects' pool at the University of Glasgow. Exclusion criteria were an Axis I psychiatric disorder according to the Diagnostic and Statistical Manual, fourth edition (DSM-IV); a diagnosis of physical illness which was ascertained based on participants' self-reported medical and medication history; a diagnosis of current infection, which was ascertained based on the presence of any self-reported symptoms suggestive of active infection; a history of *Salmonella typhi* vaccination over the last 3 years or any other vaccinations over the last 6 months; a history of antibiotic or anti-inflammatory treatment (including nonsteroidal anti-inflammatory drugs) over the last 2 weeks; a history of substance dependence or current use of tobacco; any contraindication to *Salmonella typhi* vaccination or fMRI. Participants were requested to avoid caffeinated and alcoholic beverages, high-fat meals and strenuous physical exercise for 12 hours before testing.

We only recruited male subjects in the study for various reasons. Inflammatory markers are positively associated with menstrual symptoms severity (Bertone-Johnson et al., 2014) and fluctuate throughout the menstrual cycle (Blum et al., 2005). Moreover, the use of oral contraceptives increases the level of circulating inflammatory markers (Divani, Luo, Datta, Flaherty, & Panoskaltsis-Mortari, 2015). Finally, neither a pregnancy test nor the use of contraceptives is a conclusive way of ruling out pregnancy and uncomplicated pregnancy can induce a state of low-grade inflammation (Challis et al., 2009; Palm, Axelsson, Wernroth, Larsson, & Basu, 2013; Sacks, Studena, Sargent, & Redman, 1998).

Based on a previously documented behavioural effect size ($\eta^2 = 0.96$) (Harrison et al., 2016) obtained using a similar reward learning task and the same intervention (i.e. typhoid vaccine) and randomised crossover design, we estimated a sample size of 14 subjects would give us a power of 90% at alpha=0.05 (two-tailed). We also factored in a 25% drop out rate and estimated a final total sample size of 20 subjects.

2.2 Study procedures

2.2.1 Study design

We conducted a double-blind, placebo-controlled, randomised crossover trial (https://classic.clinicaltrials.gov/ct2/show/NCT02653235) (Fig. 1). Although the study was pre-registered as a clinical trial, the behavioural task and hypotheses presented in this

manuscript were not included in the pre-registration. Each participant received placebo or typhoid vaccine on the same arm over two separate visits. The order in which the study's interventions were delivered was randomised according to a 1:1 allocation ratio. Treatment assignment was concealed, and the randomisation schedule was generated and kept within the pharmacy. Participants, investigators, and pharmacist were blind to treatment allocation, which was only revealed at the end of the study. To minimise the risk of unblinding, the syringes were prefilled, and the injections were administered by a nurse independent of the study. All visits were scheduled at 9am. While participants were not allowed to eat throughout the whole experimental session, they were allowed to drink water. Baseline IL-6 level, biological measurements and the self-rated Profile of Mood States (POMS) questionnaire were taken before participants received the injection. At 3 to 4 hours after the injection participants underwent MRI scanning, which included a resting state and a task-based fMRI scan. The results of the resting state fMRI scans have already been reported in previous papers (Stefanov, McLean, Allan, Cavanagh, & Krishnadas, 2020; Stefanov, McLean, McColl, et al., 2020). Follow-up IL-6 level, biological measurements and the POMS questionnaire were repeated after the scans. The choice of conducting behavioural, neuroimaging and other follow-up tests at 3 to 4 hours after the injection was based on prior evidence that mood scores in the placebo and typhoid vaccine groups separated out at 3 hours post injection (Wright, Strike, Brydon, & Steptoe, 2005). All participants provided written informed consent. The study protocol was approved by the West of Scotland Ethics Committee.

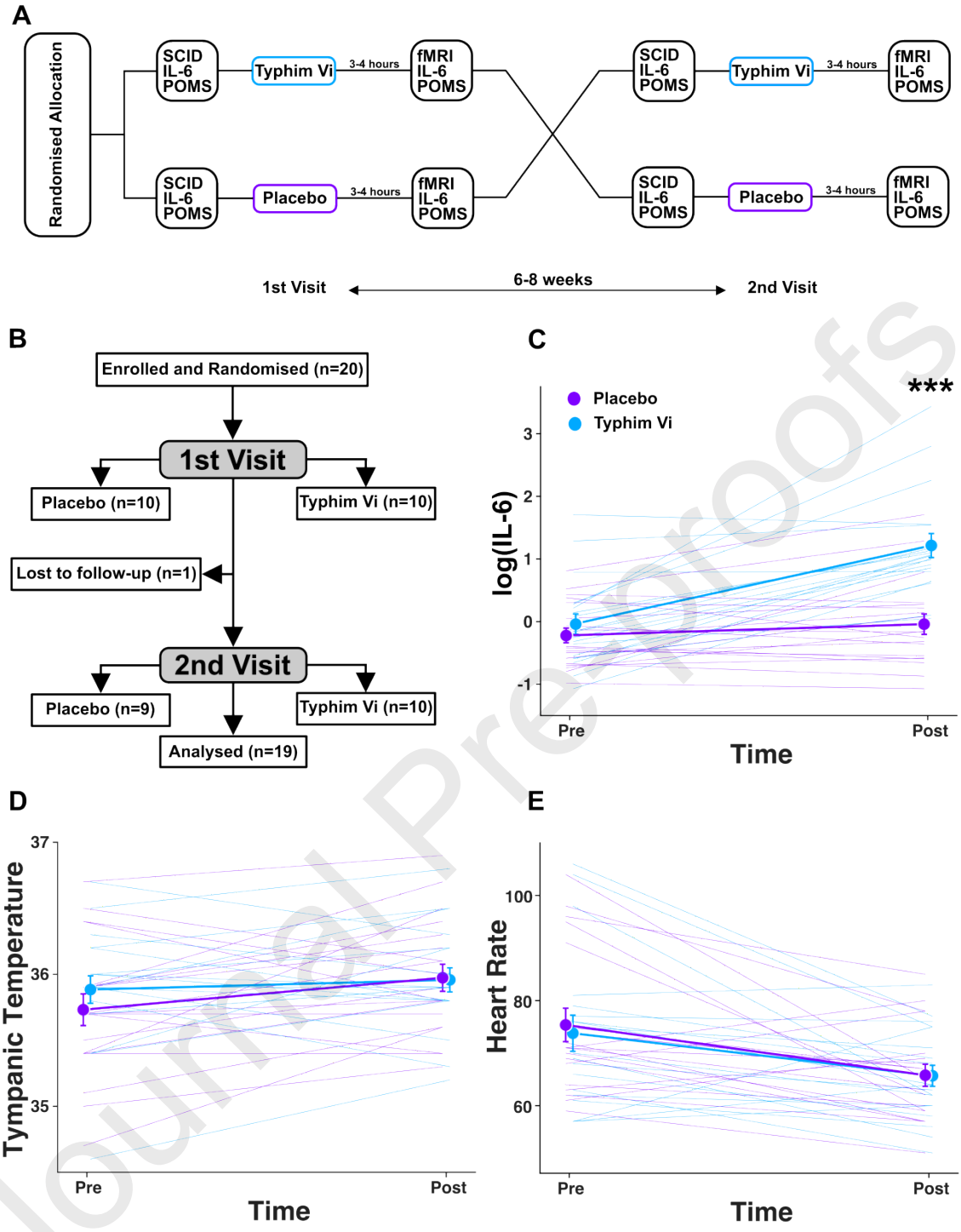

Fig. 1. Experimental design and systemic biological response. (A) The study design and experimental protocol. SCID is the Structured Clinical Interview for DSM-IV. IL-6 is interleukin 6. POMS is the self-rated Profile of Mood States questionnaire. (B) CONSORT Flow Diagram (C) Interaction plot showing significant effect of typhoid vaccine on plasma IL-6 levels as indexed by statistically significant time (pre- vs. post-injection) x condition (placebo vs. typhoid vaccine) interaction. (D-E) Interaction plots showing no significant effect of typhoid vaccine on heart rate (bpm) and tympanic temperature (°C). Means ± SEM are shown. Color-coded semi-transparent lines represent individual data. *** $p<0.001$

2.2.2 Study interventions

Salmonella typhi (Typhim Vi) vaccine consisted of the Vi capsular polysaccharide typhoid vaccine (Sanofi Pasteur Europe, Lyon, France), 50-mg/mL virulence polysaccharide antigen of formaldehyde-inactivated *Salmonella typhi*. The typhoid vaccine is a low-grade inflammatory challenge which has been shown to significantly increase IL-6 plasma levels (Brydon et al., 2009; Harrison et al., 2009; Strike, Wardle, & Steptoe, 2004; Wright et al., 2005). Crucially, the typhoid vaccine gives rise to the host of acute, transient and mild cognitive, affective, and motivational changes that are typical of sickness behaviour and resemble depressive features, without any effect on joint pain, tympanic temperature, or hemodynamic parameters (Brydon et al., 2009; Harrison et al., 2009; Strike et al., 2004; Wright et al., 2005). The placebo was 0.5 ml of isotonic saline solution.

2.2.3 Biological measurements and the POMS questionnaire

At the start of each visit all participants were screened for the presence of DSM-IV Axis I psychiatric disorders using the Structured Clinical Interview for DSM-IV. Moreover, additional baseline psychological measurements included the State-Trait Anxiety Inventory (Spielberger, 1983), the Beck Depression Inventory (Beck, Steer, & Brown, 1996) and the Functional Assessment of Chronic Illness Therapy – Fatigue Scale (Webster, Cella, & Yost, 2003) to screen for any baseline trait and state anxiety, subclinical depression and severe fatigue.

On each visit patients completed the POMS questionnaire (McNair, 1971) at baseline and 3 to 4 hours post-injection. The POMS is a validated self-rated psychometric scale designed to assess transient mood symptoms and is thus sensitive to the cognitive, affective and motivational changes associated with inflammation-induced sickness behaviour. The POMS is made up of 65 items grouped in 6 different subscales assessing different mental state dimensions such as Tension-anxiety, Depression-dejection, Anger-hostility, Fatigue-inertia, Confusion-bewilderment and Vigour-activity. The Total Mood Disturbance score is calculated by subtracting the Vigour-activity score from the total obtained from adding up the scores of the other subscales.

Tympanic temperature, heart rate, blood pressure and plasma IL-6 level were measured at baseline and 3 to 4 hours post-injection. Moreover, at 3 to 4 hours post-injection a research nurse ascertained whether participants reported any pain or discomfort at the injection site and visually inspected the injection site for the presence of swelling. To measure plasma IL-6 level a sample of 10 mL of venous blood was drawn into BD Vacutainers (BD Biosciences, Franklin Lakes, NJ) containing K2EDTA and centrifuged immediately at 8000 rpm for 10 minutes. Plasma was collected and frozen at -80°C. IL-6 was assayed in duplicate using Human IL-6 Quantikine High-Sensitivity ELISA kits (R&D Systems, Minneapolis, MN) as per

the manufacturer's instruction. Optical densities were read using an Infinite 200 PRO TECAN microplate reader (Tecan, Männedorf, Switzerland) and were converted into concentrations against a 7-point standard curve. The kit sensitivity was 0.11 pg/mL and the intra- and inter-assay coefficients of variation were 10% and 11%, respectively. There were no IL-6 values below the detection limit. Furthermore, based on the finding of a previous meta-analysis that the pooled estimate of IL-6 values in the blood of healthy adult donors (n=3166) was 5.186 pg/ml (95% confidence interval: 4.631, 5.740) (Said et al., 2021), we considered any baseline IL-6 value exceeding the upper 95% confidence interval limit (i.e. 5.74 pg/ml) as indicative of possible active infection. We did not find any baseline IL-6 values in our sample to be greater than this cut-off.

2.2.4 Behavioural task

In the fMRI experiment we employed a PRL task (n=180), which is shown in Figure 2 and was previously described in (Fouragnan, Queirazza, Retzler, Mullinger, & Philiastides, 2017; Fouragnan, Retzler, Mullinger, & Philiastides, 2015; Queirazza, Fouragnan, Steele, Cavanagh, & Philiastides, 2019). Briefly, participants were required to choose between two abstract visual stimuli, which were randomly sampled from a pool of 18 different geometrical shapes. Both stimuli could yield either a positive (+10) or negative (−10) outcome devoid of monetary value. Reinforcement contingencies were probabilistic and asymmetrically skewed so that one stimulus (i.e. the high probability stimulus) had a greater chance of yielding a positive outcome than the other stimulus (i.e. the low probability stimulus). Reversals of reinforcement contingencies were triggered when participants chose the high-probability stimulus five times over the last six trials. As a result, participants experienced a different number of reversals. Furthermore, to prevent participants from easily figuring out the underlying reversal rule, we ran a randomly generated number of buffer trials from a zero-truncated Poisson distribution before reversing stimulus-outcome contingencies.

Participants were advised of the probabilistic nature of the task and that reinforcement contingencies might reverse based on their performance. They were also advised the goal of the task was to get as many positive outcomes (i.e. +10) as possible and that their performance would be monitored. Moreover, to allow participants to familiarise themselves with the nature of the task, they had a 5-minutes practice session before the fMRI scan. The task was programmed using Presentation (Neurobehavioural Systems) stimulus delivery software. Participants were remunerated at the end of each experimental session for their participation, including their daily and travel allowance (up to £100).

The PRL task is ideally suited to probing biases in the acquisition and processing of feedback during probabilistic learning. Optimal performance rests on the subjects' ability to infer whether fluctuations in the observed stimulus-outcome associations reflect either noise (given the stochastic reinforcement schedule) or sudden environmental changes (that is, reversals).

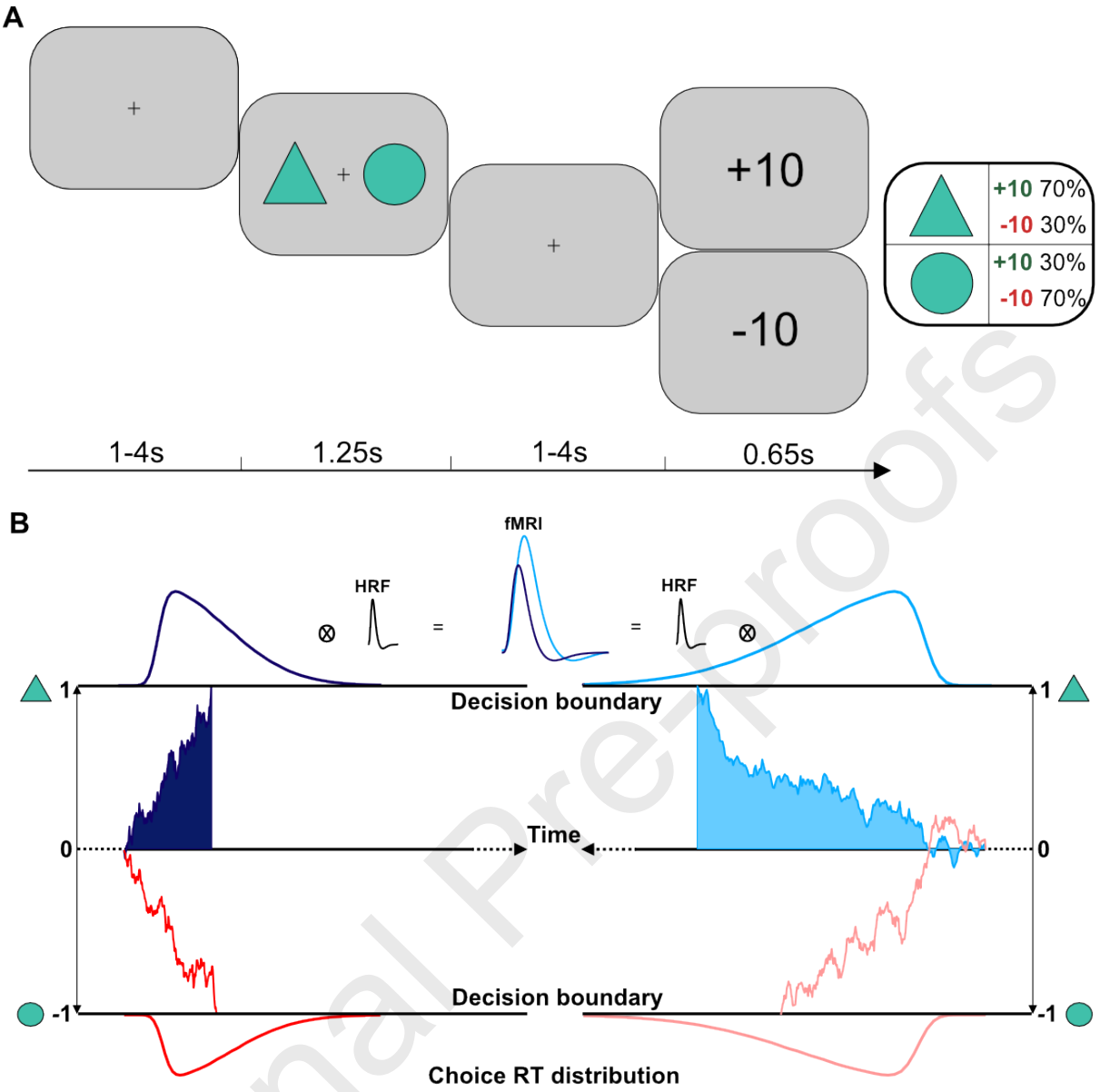

Fig. 2. Behavioural task and computational model. (A) Probabilistic reversal learning task. Each trial commenced with a jittered interstimulus interval (1 to 4 s) displaying a fixation cross. Subsequently, two geometrical shapes appeared randomly on either side of the screen for 1.25 s. Participants had 1 s to make a choice via a button press. In case of late responses participants were presented with a screen prompting them to respond faster. Following a second jittered interstimulus interval (1 to 4 s), participants were presented with the outcome of their decision for 0.65 s. Outcome was either positive (+10) or negative (−10). Reinforcement contingencies were asymmetrically skewed (70 to 30%) so that the expected value of the two stimuli was of the same magnitude but of opposite sign. To maximize the design efficiency for the fMRI analysis, the duration of jittered interstimulus intervals was optimized using a genetic algorithm. (B) Short (dark blue/red) versus long (light blue/red) integration time. We modelled the decision phase of the task using an OU process. Solid red and blue traces represent moment-by-moment ramping up of decision evidence at slow (right) and fast (left) accumulation rates indexing decisions of low and high discriminability respectively. Magnitude of accumulation rates was determined by difference of expected values (as a proxy measure of subjective decision discriminability),

'urgency' to make decision and stochasticity inherent to decision process (that is, noise). Shaded areas under EA ramps denote short (dark blue/red) versus long (light blue/red) integration times. Convolution of short versus long AUCs (that is, area under EA curves) with a hemodynamic response function (HRF) yields low versus high predicted BOLD activity respectively. Dotted black line represents non-decision time.

2.3 Computational modelling

2.3.1 Model architecture

To provide a fine-grained mechanistic account of the decision-making processes underlying observed choice behaviour during the PRL task we devised nested hybrid RL and SSM computational models (Pedersen et al., 2017). Based on prior empirical findings that integration of decision evidence is a domain-general mechanisms also pertaining to value-based decisions (Krajbich et al., 2010; Pisauro et al., 2017), we mathematically described the decision phase of the task using an Ornstein-Uhlenbeck (OU) process (Arabadzhiyska et al., 2022; Pisauro et al., 2017; Polania, Krajbich, Grueschow, & Ruff, 2014) as the choice rule. The OU process is a variant of the leaky competing accumulator family of models (Bogacz, Brown, Moehlis, Holmes, & Cohen, 2006). It assumes that a decision is made by accumulating noisy evidence via a single integrator (i.e. decision unit) until a decision boundary is reached in favour of one of two alternatives. Within each trial decision evidence is continuously updated as per the following equation:

$$EA_{t+1} = EA_t + (\lambda EA_t + \kappa DV_k)dt + \sigma dW_t$$

where EA is the amount of evidence accumulated at time t, DV denotes the signed decision variable's magnitude at trial k (that is, the trial-by-trial difference between choice values Q^1 and Q^2) thus indexing choice discriminability (i.e. difficulty), dW represents independent (Wiener) white noise fluctuations at time t thus accounting for RT within-trial variability and dt is the sampling timestep, which was set to 0.001s. The free parameter κ denotes sensitivity to choice discriminability and can be interpreted as the individual ability to discern decision evidence. While the free parameter λ represents the 'urgency' to reach the decision boundary, the free parameter σ scales the inherent noisiness corrupting decision evidence accumulation. Moreover, we included a lag parameter nDT, which accounts for non-decision time processes including encoding of visual stimuli and motor preparation/execution. Unless otherwise specified we assumed that a decision is made when $|EA|$ is 1. Response times are estimated by the time EA takes to reach the decision threshold plus the non-decision time nDT. We assumed the starting point was 0 and thus unbiased. The DV determines the average rate of evidence accumulation per unit of time operating as a dynamic drift rate. Crucially, we estimated the efficiency of decision evidence integration by computing the area under the curve (AUC) of trial-wise *EA* ramps to quantitatively model the efficiency of neural processing of decision evidence as a function of

perceived choice discriminability (Figure 2B) (Pisauro et al., 2017). Short integration times are determined by steeper *EA* ramps, which are on average associated with greater *DV* values thus indexing (subjectively) more discriminable and therefore less 'effortful' decisions. Conversely, long integration times result from shallow *EA* ramps that are linked to smaller *DV* values denoting (subjectively) less discriminable and therefore more 'effortful' decisions.

Choice values Q^1 and Q^2 are updated according to a conventional Rescorla-Wagner learning rule:

$$Q^i_{k+1} = Q^i_k + \alpha(R_k - Q^i_k)$$

where R is the feedback received at trial k and superscript $i \in [1,2]$ indicates the chosen Q value at trial k. The difference between feedback R and expected Q value represents the RPE. The free parameter α is the learning rate. We tested 3 differently parameterised models, which are illustrated in Table 1. In the RLSSM1 model we fixed the parameters σ to increase model's parsimony. In the RLSSM3 model we allowed the decision bound to vary across participants as the free parameter a. A higher decision bound reflects slower but more accurate decisions and vice versa. A major advantage of our hybrid modelling approach is that combining RL and SSM models accounts for both within-trials (i.e. ramping up of decision evidence) and across-trials (i.e. feedback-based updating of the decision variable) decision dynamics.

	nDT	λ	κ	α	σ	*a*
RLSSM1	3.25±1.03	1.89±0.36	1.18±0.6	-1.81±1.74	**1**	**1**
RLSSM2	√	√	√	√	√	×
RLSSM3	√	√	√	√	×	√

Table 1. Models' parameters. We fitted 3 differently parameterised models to observed RTs and choice data. Mean ± standard deviation of fitted parameters in their native space are shown for the best fitting model. Bold fonts (and red crosses) indicate fixed parameters.

2.4.2 Model fitting

For each subject *j* we fitted a computational model to the observed choices and RT distributions and estimated the negative log likelihood NLL using the following cost function:

$$NLL_j = -[log(KS(RT_{data}^{choice\ 1}, RT_{model}^{choice\ 1})) + log(KS(RT_{data}^{choice\ 2}, RT_{model}^{choice\ 2}))]$$

where $KS(x,y)$ is the Kolmogorov-Smirnov test (*kstest2* function in Matlab) estimating the probability that x and y come from the same continuous distribution.

To optimise model parameters, we initially performed a search over a coarse grid of values and identified the subject-specific set of parameter values minimising the NLL cost function. For each parameter we set an upper and lower grid bound (κ [0.5,3], λ [1,3], σ [-0.5,2], nDT [1,5], α [-4,4], a [-1,0]) in the parameters' native space and then sampled 20 equally spaced values including the grid bounds. To enforce the parameters natural bounds, we implemented log (κ, λ, σ, nDT, a) and logit (α) transforms of the parameter values. We then used the parameter values obtained from the grid search to initialise a quadratic optimisation routine (*fminunc* function in Matlab) and derived the best fitting set of parameter estimates.

2.3.3 Model comparison and validation

To perform formal model comparison, we estimated the Bayesian Integration Criterion (BIC) as follows:

$$BIC = \sum_{j}^{N} 2NLL_j + dlog(T_j)$$

where T is the total number of trials for subject *j* and d is the number of free parameters.

To evaluate the models' ability to reproduce observed response latency and accuracy, we correlated fitted and observed subject- and choice-wise mean RTs and accuracy using 20% bend correlation test (Pernet, Wilcox, & Rousselet, 2012).

2.4 fMRI

2.4.1 fMRI data acquisition

We used a 3T GE system with an eight-channel parallel imaging head coil. We acquired a high-resolution T1-weighted structural image (0.5 mm by 0.5 mm by 1.2 mm voxels, 512 by 512 matrix, 124 axial slices, inversion time (TI) = 450 ms, repetition time (TR) = 7700 ms, echo time (TE) = 1.5 ms, flip angle = 12°) using an optimized inversion recovery fast spoiled gradient echo sequence and a functional echo planar imaging scan (3-mm isotropic voxels, 64 by 64 matrix, 608 axial slices, TR = 2000 ms, TE = 30 ms, flip angle = 80°). Slice orientation was tilted to +30° from the anterior commissure-posterior commissure (AC-PC) plane to reduce signal dropout in the orbitofrontal cortex (Weiskopf, Hutton, Josephs, & Deichmann, 2006). The first four volumes of the functional scan were discarded to allow for the magnetic field to reach the steady state.

2.4.2 fMRI data preprocessing

fMRI data preprocessing and statistical analyses were performed using FSL (FMRIB's software library) software. Preprocessing pipeline involved intramodal motion correction using MCFLIRT (motion correction FMRIB's linear image registration tool), slice timing correction, spatial smoothing with an isotropic 5-mm full width at half maximum Gaussian kernel, high-pass temporal filtering with a cut-off frequency of 110 s, and grand-mean intensity normalization of each entire four-dimensional dataset. Functional scans were subsequently coregistered with skull-stripped structural images using boundary-based registration as implemented in FLIRT (FMRIB's linear image registration tool) and spatially normalized into MNI152 space using FNIRT (FMRIB's non-linear image registration tool) nonlinear registration.

2.4.3 fMRI data analysis

We performed whole-brain statistical analyses using a multilevel mixed-effects approach as implemented in FLAME1 (FSL). Our choice to conduct whole-brain analyses was motivated by the distributed nature of the brain networks exhibiting EA dynamics during decision making (Gherman et al., 2024). Importantly, we implemented a model-based fMRI approach (O'Doherty, Hampton, & Kim, 2007), where the regressors of interest were continuous parametric regressors derived from the model fit. At the first level, we built a design matrix modelling both the decision and outcome phases of the behavioural task.

To probe the effect of inflammation on the efficiency of decision dynamics such as bounded evidence accumulation we investigated brain activity covarying with the trial-wise AUC estimates of the fitted EA ramps. The model-derived AUC estimates reflect the level of underlying aggregate activity of pools of neurons involved in stimulus value integration and should therefore scale with BOLD responses in regions of the brain that operate as evidence

accumulators (that is, as shown in Figure 2B, greater BOLD responses for long integration time and vice versa). More specifically, we reasoned that inflammation may differentially impact neural integration of decision evidence at different timescales (short versus long integration time) and thus as a function of perceived choice discriminability. To test this hypothesis, we modelled the interaction effect of evidence integration time (short versus long) and experimental condition (placebo versus typhoid vaccine) on the neural accumulation of decision evidence. At the first level we set up a contrast (i.e. short – long evidence integration time) to capture the (simple) effect of evidence integration time in the placebo and typhoid conditions. At the second level, we tested for a significant between-condition difference of the simple effects.

In the main analysis we built a design matrix where we derived two parametric regressors by performing a median split of the fitted AUC estimates so that while one regressor modelled "long" EA processes (that is, equal to/greater than median AUC value), another regressor modelled "short" EA processes (that is, smaller than median AUC value). We also included a nuisance regressor, which was modulated by the reaction times and thus accounted for both visual stimulation and motor response. All the regressors in the decision phase were aligned with the onset of the decision phase**.** In a supplementary analysis we used a single parametric regressor for accumulated evidence in the design matrix. The goal of this supplementary analysis was to test for any significant effect of typhoid vaccine on the neural encoding of decision evidence accumulation independent of integration time.

The regressors in the outcome phase were aligned with the onset of the outcome phase and included a parametric regressor of interest encoding the trial-wise model-derived RPE estimates and two unmodulated nuisance regressors representing visual stimulation and lost trials respectively. We included six additional motion parameters (three translations and three rotations) estimated during the motion correction phase as regressors of no interest. We modelled all regressors as stick functions. We ensured that our design matrix was well conditioned and not rank deficient using the collinearity diagnostics incorporated in FSL. We convolved all regressors with a hemodynamic response function (double gamma function).

To test for any significant between-condition (placebo versus typhoid vaccine) differences we conducted a second-level mixed-effects analysis of the subject-wise linear contrasts of the parameter estimates using a paired two-sample t test. We thresholded the resulting Z statistic images using a cluster-defining threshold of $Z > 2.57$ and an FWE-corrected significance threshold of $P = 0.05$.

2.5 Statistical analyses

2.5.1 Biological measurements and POMS scores

To identify outlying IL-6 values we calculated the z-score of the pre- and post-injection IL-6 values in both the typhoid vaccine and placebo conditions and considered any z-score equal to or greater than 3 as an outlier. We identified two IL-6 outlying values in the typhoid vaccine condition. We applied a log-transformation to treat outlying IL-6 measures and correct positively skewed data. To test for any significant between-condition differences in the pre- to post-injection mean change of log(IL-6), biological measurements and POMS scores we conducted 2x2 repeated measures ANOVA using factors condition and time as the independent variables and examining the condition x time interaction.

2.5.2 Behaviour and model parameters

To analyse observed choice behaviour during the task we conducted maximal by-subject random intercept and random slopes generalised and loglinear mixed-effects models (Barr, Levy, Scheepers, & Tily, 2013) using the *lme4* package in R (http://www.r-project.org) and allowing for random correlations between independent variables. We tested the statistical significance of the fixed effects using the likelihood ratio test (Barr et al., 2013).

To test task related learning effects as a function of the experimental *condition* (placebo versus typhoid vaccine) we conducted the following mixed-effects regression model:

$$logit(choice) = 1 + hps * condition + (1 + hps * condition|subject)$$

where *hps* denotes the high probability symbol. A positive main effect of the high probability symbol on choice behaviour suggests a learning effect on task performance. The interaction term captures the effect of typhoid vaccine on task performance.

Furthermore, we ascertained whether there was any typhoid-dependent feedback valence (*fbk*) effect on the probability of repeating same choice (*stay*) and response times (*RT*) as per the following models:

$$logit(stay) = 1 + fbk * condition + (1 + fbk * condition|subject)$$

$$log(RT) = 1 + fbk * condition + (1 + fbk * condition|subject)$$

To test for any significant between-condition differences in behavioural measures (including mean accuracy and median RT) and model parameters we conducted the following linear regression model:

$$vcn_j - plb_j = 1 + order_j + \overline{plb_j}$$

where the intercept represents the between-condition mean difference adjusted for potential order effect. The factor *order* indexes whether, for subject j, typhoid vaccine was administered during the first or second visit and the term $\overline{plb}$ is the mean-centred placebo score, here used as a covariate to reduce sampling variance and increase statistical power (Hedberg & Ayers, 2015).

3. Results

3.1 Participants

We recruited twenty healthy male participants. One participant advised he had been diagnosed with clinical depression and commenced on antidepressant treatment during his second visit and was thus excluded from the study sample. Otherwise, we did not find evidence of Axis I psychiatric disorder, trait and state anxiety, subclinical depression and severe fatigue for the remaining participants. The sample mean age was 25.63 ± 6.52 years and the sample mean BMI was 22.76 ± 2.17.

3.2 Biological measurements and POMS scroes

Typhoid vaccine significantly raised IL-6 plasma levels (condition x time interaction: $F_{1,18}$=31.4, p<.001) as shown in Figure 1C. Typhoid vaccine was not associated with a significant change in tympanic temperature (condition x time interaction: $F_{1,18}$=1.18, p=.29) (Figure 1D), heart rate (condition x time interaction: $F_{1,18}$=.321, p=.57) (Figure 1E), systolic (condition x time interaction: $F_{1,18}$=.008, p=.93) or diastolic (condition x time interaction: $F_{1,18}$=1.69, p=.21) blood pressure. Moreover, none of the participants reported any discomfort or pain, or exhibited swelling on the injection site at 3 to 4 hours post-injection, all of which minimised the risk of unblinding.

We did not find any statistically significant effect of the condition x time interaction on POMS total and sub scores (total POMS: $F_{1,18}$=.85, p=.37; depression: $F_{1,18}$=.008, p=.93; fatigue: $F_{1,18}$=3.4, p=.08; vigour: $F_{1,18}$=.28, p=.6; tension: $F_{1,18}$=.008, p=.93; confusion: $F_{1,18}$=.61, p=.45; anger: $F_{1,18}$=.65, p=.43). While failing to reach statistical significance, severity of fatigue symptomatology was greater in the typhoid vaccine condition and was

557 the most pronounced behavioural difference as a function of inflammation. Raw biological
558 measures and POMS scores are shown in Table 2.

559

	Placebo (pre)	*Placebo (post)*	*Vaccine (pre)*	*Vaccine (post)*
Biological measures				
IL-6 (pg/ml)	0.91±0.51	1.21±0.89	1.28±1.28	5.26±7.19
Tympanic temperature (°C)	35.73±0.52	35.97±0.45	35.88±0.45	35.96±0.40
Systolic pressure (mmHg)	120.47±9.94	122.11±6.65	120.21±11.39	121.47±7.10
Diastolic pressure (mmHg)	78.47±7.50	75.26±7.10	76.11±8.81	75.74±7.82
Heart rate (bpm)	75.37±13.86	65.79±9.20	73.79±14.97	65.68±8.70
POMS				
Tension - anxiety	11.26±2.16	10.32±1.6	11.26±2.42	10.37±1.83
Depression – dejection	15.58±1.12	15.37±0.96	15.79±1.36	15.63±2.52
Anger – hostility	13.05±2.15	12.84±1.46	13.37±2.77	12.84±1.38
Vigour – activity	26.37±5.06	24.95±6.15	27.32±4.97	25.05±7.79
Fatigue – inertia	9.32±2.52	8.37±2.03	9.68±2.81	10.37±4.02

Confusion - bewilderment	10.74±1.52	10.37±1.12	10.58±1.54	10.53±2.14
Behavioural Task				
Accuracy rate		0.66±0.07		0.64±0.1
Reaction time (seconds)		0.65±0.07		0.64±0.07

Table 2. Raw biological measurements, POMS scores and behavioural results. Mean ± standard deviation are shown for data collected before (pre) and after (post) injection.

3.3 Model comparison and fit

On formal model comparison we found that the most parsimonious model RLSSM1 provided the best fit to observed behaviour (BIC=569) compared to RLSSM2 (BIC=694) and RLSSM3 (BIC=704) (Figure 3A). Moreover, we found that RLSSM1 was able to reproduce observed behavioural effects as across subjects correlations between fitted and observed mean RT and choice accuracy were statistically significant (Figure 3B-C). Taken together, these results show that both predictive and generative performance of our best fitting model is robust and thus validate such model as an accurate description of the cognitive processes underpinning decision making and learning during the task (Palminteri, Wyart, & Koechlin, 2017).

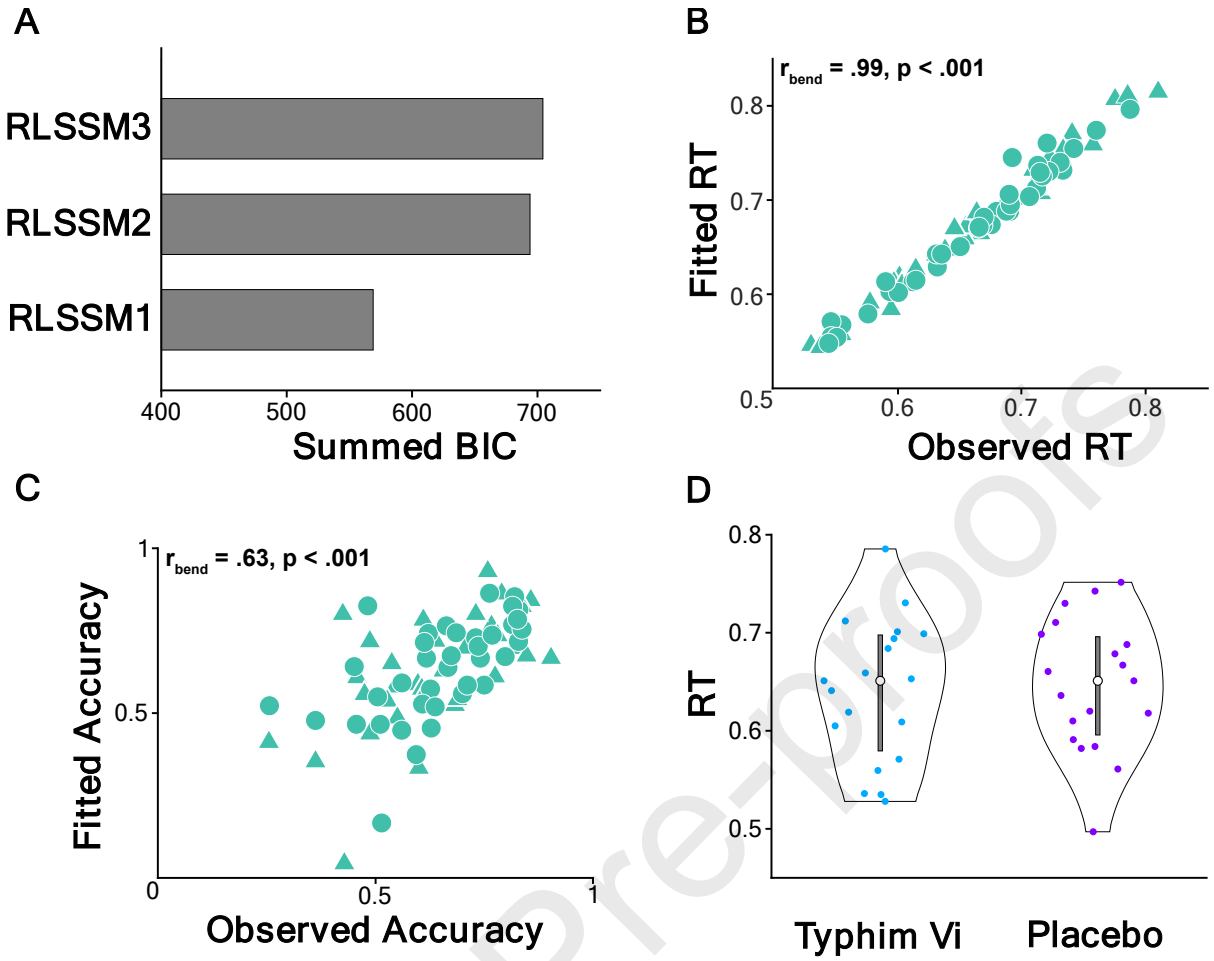

574

575 **Fig 3. Model checking and behavioural results.** (A) Model comparison showing BIC (less is
576 better). (B-C) Scatter plots (n=76) showing the relationship between subject-wise fitted and
577 observed mean choice reaction times in seconds (B) and mean choice accuracy (C). (D) Violin
578 plot showing non-significant between-condition comparison of reaction times (RT) in
579 seconds. Grey line represents interquartile range and white circle denotes the median. Light
580 blue (n=19) and purple (n=19) dots represent individual subjects. r_{bend} stands for 20% bend
581 correlation coefficient.

582

583 *3.3 Behaviour and model parameters*

584 On average participants performed above chance level during the task (main effect of hps: β
585 = 1.34, p < .001) although there was no significant effect of typhoid vaccine on task
586 performance (interaction effect of hps:intervention : β = -.11, p = .45). Positive feedback
587 significantly increased the probability of repeating same choice (β = 3.28, p < .001) but not
588 the speed of button presses (β = .003, p = .81) on subsequent trials. There was no significant
589 typhoid dependent effect of feedback on choice perseveration (β = -.25, p = .40) and
590 response times (β = -.01, p = .59). We did not find typhoid vaccine to have any significant
591 effect on behavioural variables recorded during the RL task including response latencies
592 (t_{16}=1.18, p=.25) (Figure 3D) and choice accuracy (t_{16}=.84, p=.42) (Table 2). Likewise, there
593 were no statistically significant between-condition differences in the best-fitting model

parameters estimates (nDT : t_{16}=.87, p=.39; α : t_{16}=.85, p=.41; λ : t_{16}=.89, p=.38; κ : t_{16}=.71, p=.49) (Figure 4). Thus, typhoid vaccine did not have a significant effect on non-decision time (*nDT*), the step size of choice value update (α), the 'urgency' to make a decision (λ) and the individual ability to discern decision evidence (κ). It is possible that the lack of significant behavioural and computational effects of the typhoid vaccination was due to i) the low-level inflammatory response and ii) insufficient power because of the relatively small sample size.

Previous studies documented significant behavioural findings in the context of low-grade inflammation, albeit employing different behavioural and experimental paradigms. Harrison et al. found that typhoid vaccination enhanced punishment but attenuated reward sensitivity during a reinforcement learning task (Harrison et al., 2016). However, in their task punishment and reward learning were tested in separate sessions and stimulus-outcome contingencies were not reversed. Boyle et al. reported that the probability of choosing the more frequently rewarded of two stimuli (that is, reward responsiveness) in a popular (implicit) reward learning task (Pizzagalli, Jahn, & O'Shea, 2005) was positively correlated with IL-6 plasma concentrations following acute stress (Boyle, Stanton, Eisenberger, Seeman, & Bower, 2020) and influenza vaccination (Boyle et al., 2019). Though, reward sensitivity, as indexed by a computational parameter scaling reward magnitude, was not associated with IL-6 plasma concentrations (Boyle et al., 2019). Crucially, reward responsiveness reflects a reward-induced (implicit) response bias that is not captured by our task. We thus argue that the lack of behavioural findings in our study compared to previous work is primarily due to various significant methodological differences.

We thus ascertained whether fMRI data provided additional explanatory power to reveal the hypothesised (most likely subtle) effects of typhoid-induced inflammation on decision dynamics.

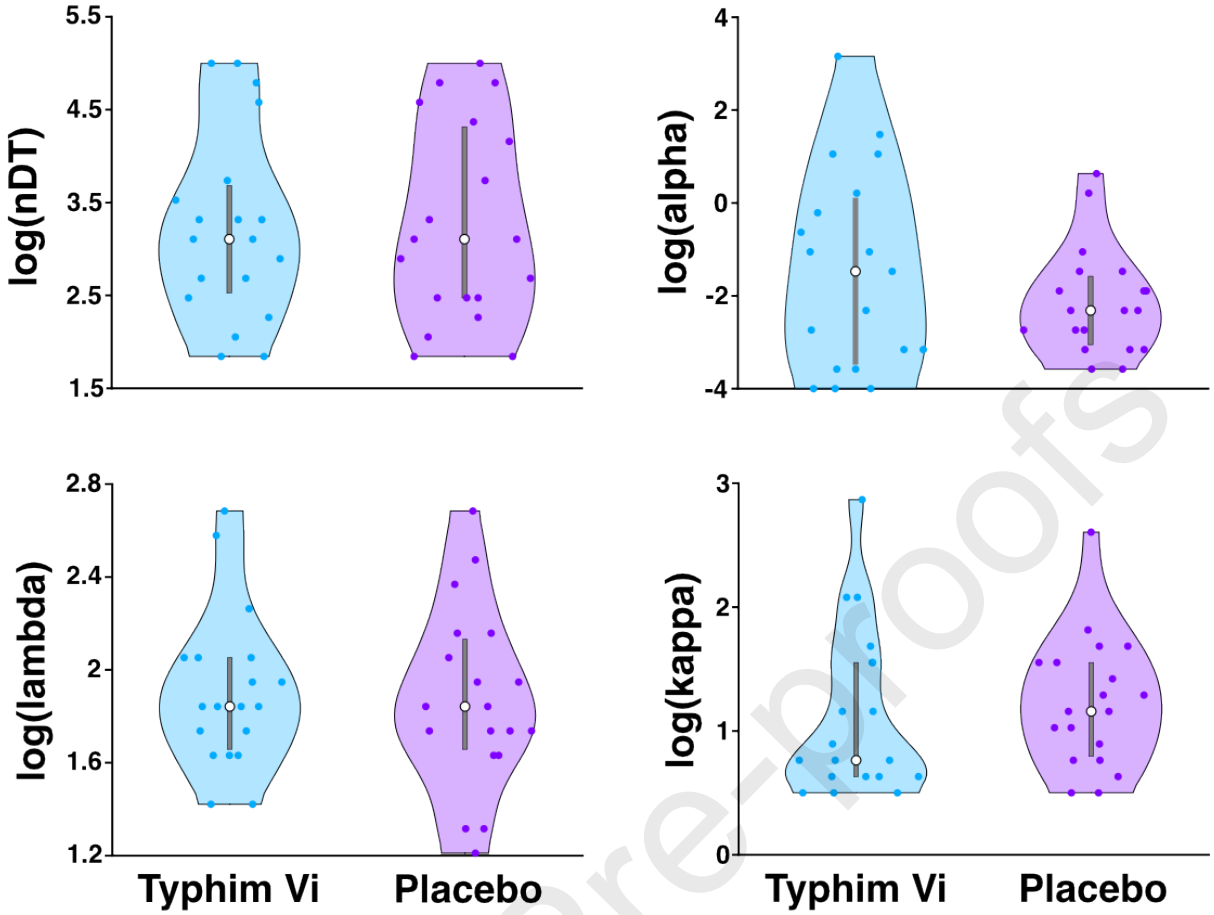

Fig. 4. Fitted parameters. Violin plots showing fitted estimates of model parameters (in their native space) as a function of experimental condition. We did not find any between-condition significant differences. Grey line represents interquartile range and white circle denotes the median. Light blue (n=19) and purple (n=19) dots represent individual subjects. nDT stands for non-decision time parameter.

3.4 fMRI

3.4.1 Model-based fMRI analysis

In the decision phase of the reward learning task, we found a significant interaction effect of evidence integration time and experimental condition on the neural accumulation of decision evidence in the dorsomedial prefrontal cortex (dmPFC) bilaterally (peak Z score = 3.7; MNI space coordinates = 0,50,34; $p < .05$ FWE) (Figure 5A). Conversely, we did not find any evidence that the typhoid vaccine had a significant effect on BOLD activity covarying with the accumulation of decision evidence independent of integration time. As shown in Figure 6, the interaction effect was primarily driven by typhoid-induced attenuation of BOLD activity representing short EA processes. Moreover, we did not observe a monotonic effect of integration time on the dmPFC haemodynamic responses in the placebo condition. Correspondingly, dmPFC activity significantly correlated with post-injection log(IL-6) plasma concentrations in the typhoid vaccine but not the placebo condition (Figure 5C). In our task we did not experimentally manipulate different levels of stimulus discriminability (or

difficulty) to explicitly modulate evidence integration times and associated haemodynamic responses. It is thus possible that the variability of EA-evoked BOLD responses in the placebo condition was insufficient to reveal a monotonic effect of integration time. Taken together, these results seem to suggest that low-grade inflammation differentially affect neural integration of decision evidence diverting neural recruitment away from decisions which are subjectively perceived as more discriminable and thus easier to integrate. We interpret this finding as evidence that transient mild inflammation re-prioritises allocation of neuronal resources away from decisions that are easier to integrate in the service of energy preservation.

At the time of outcome, we found that BOLD activity covarying with the fitted model-derived RPE estimates was significantly lower in the vaccine compared to the placebo condition as shown in Figure 5B. Typhoid vaccine attenuated RPE signals in the bilateral putamen (peak Z score = 3.69; MNI space coordinates = -28,-2,-10; $p < .05$ FWE), bilateral amygdala (peak Z score = 3.71; MNI space coordinates = -26,-2,-24; $p < .05$ FWE), bilateral hippocampus (peak Z score = 3.6; MNI space coordinates = 22,-8,-28; $p < .05$ FWE), bilateral parahippocampus (peak Z score = 3.96; MNI space coordinates = -28,-30,-22; $p < .05$ FWE) and left supramarginal gyrus (peak Z score = 3.6; MNI space coordinates = -54,-42,22; $p < .05$ FWE). Moreover, BOLD activity in the RPE cluster was more significantly associated with post-injection log(IL-6) plasma concentrations in the typhoid vaccine than in the placebo condition (Figure 5D). Our findings replicate previous reports of inflammation-induced blunting of striatal RPE signals (Harrison et al., 2016; Treadway et al., 2017).

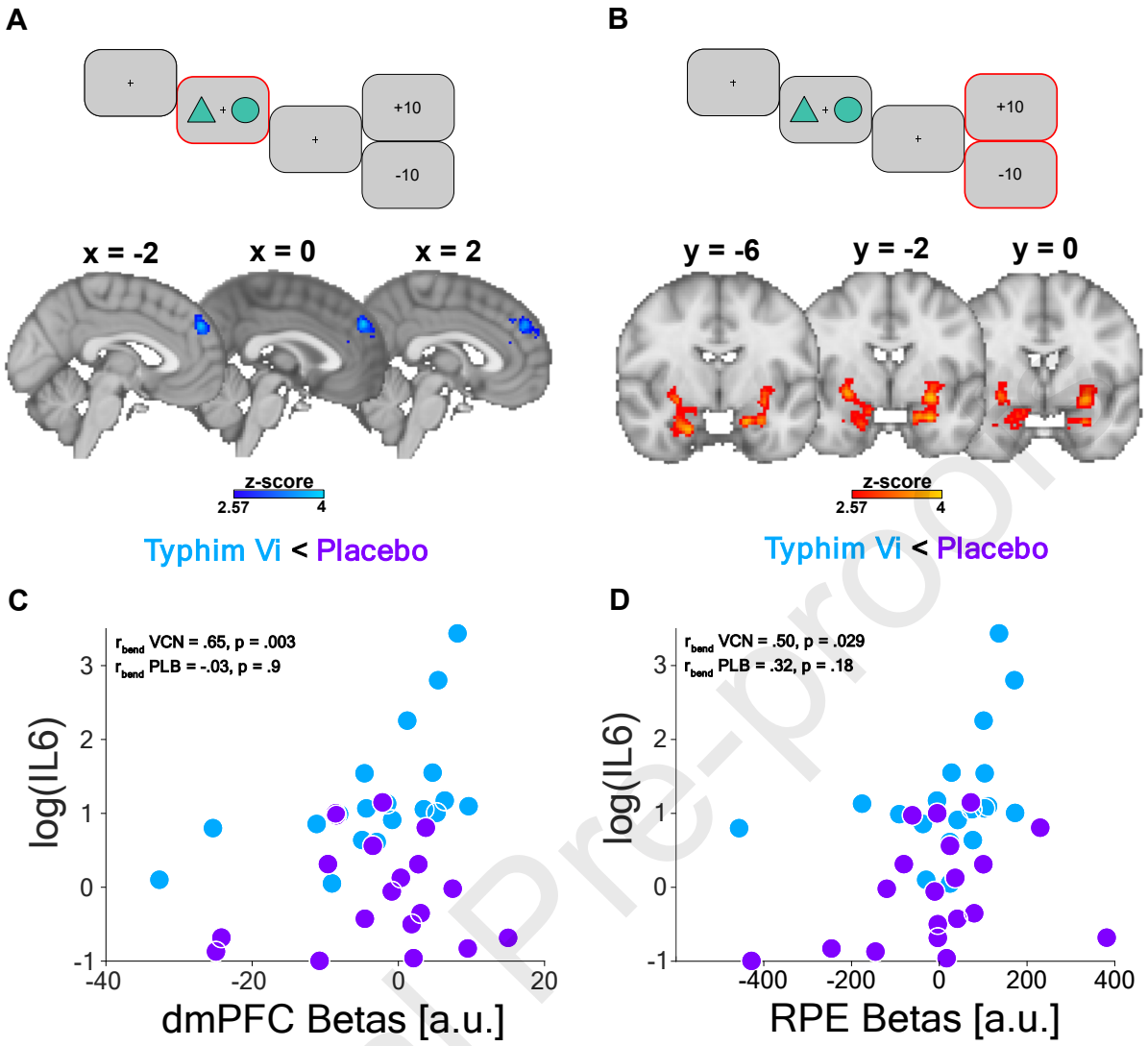

Fig. 5. fMRI results. (A) During the decision phase BOLD activity in the bilateral dmPFC denoted a significant interaction effect of evidence integration time (IT) and experimental condition on the neural accumulation of decision evidence as tested by the contrast Short IT_{VCN} – Long IT_{VCN} < Short IT_{PLB} – Long IT_{PLB}. (B) During the outcome phase BOLD activity in the bilateral putamen and amygdala/hippocampus complex encoding the RPE was attenuated in the vaccine compared to the placebo condition. MNI coordinates are shown. $p < .05$ FWE. (C-D) Scatter plots (n=38) showing correlations between post-injection log(IL-6) plasma concentrations and average parameter estimates (i.e. beta weights) extracted from the dmPFC (C) and the RPE cluster (D). Light blue and purple dots represent individual subjects in the typhoid vaccine and placebo condition respectively. r_{bend} indicates the 20% bend correlation coefficient.

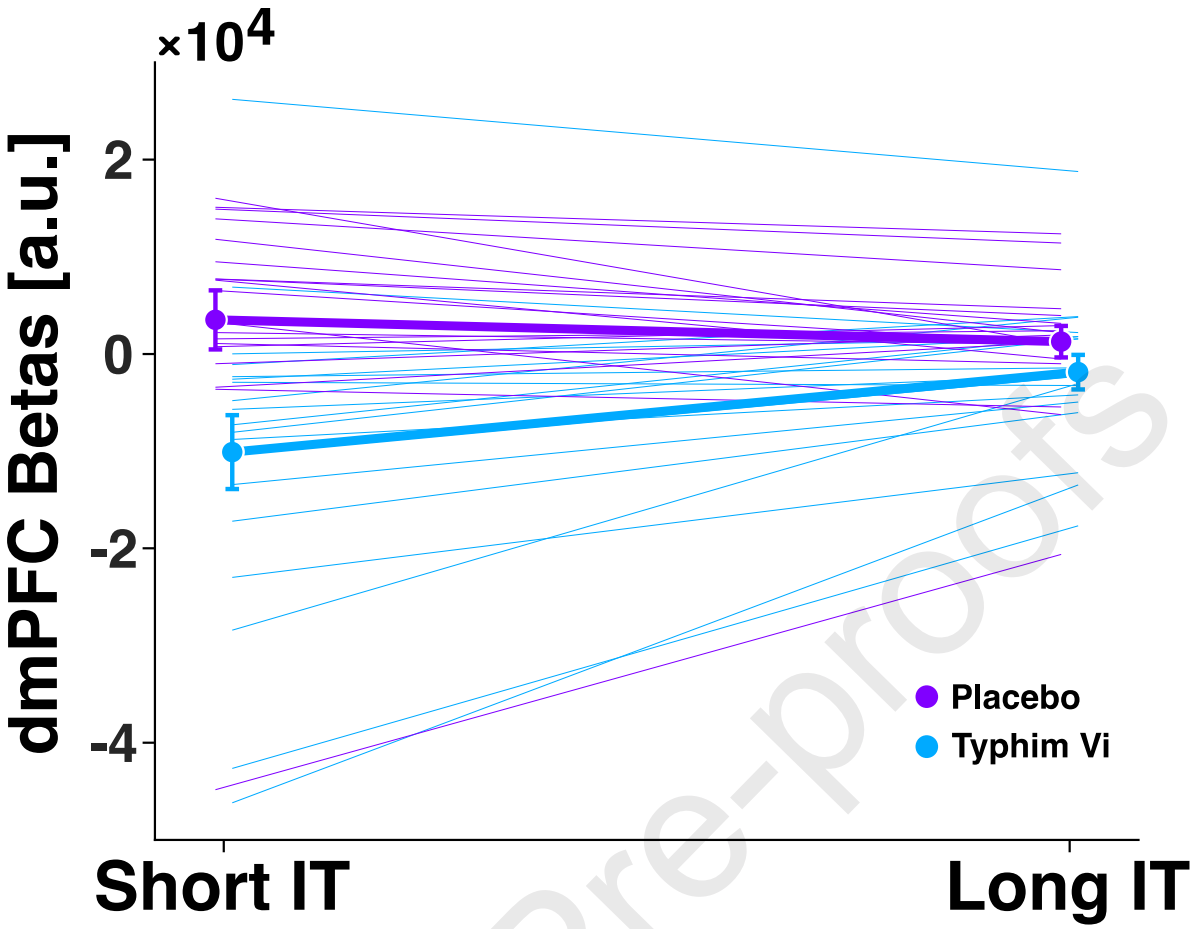

Fig. 6. Interaction plot showing the significant effect of typhoid vaccine on dmPFC beta weights as a function of evidence integration time (IT) (i.e. short versus long). Means ± SEM are shown. Color-coded semi-transparent lines represent individual data.

4. Discussion

Our data showed that acute low-grade inflammation diminishes neural activity linked to the accumulation of decision evidence in the dmPFC as a function of perceived decision discriminability. We have thus offered novel mechanistic evidence suggesting that inflammation interferes with the efficiency of neural accumulation of evidence in the decision process itself. We leveraged the insights afforded by a hybrid RL and SSM computational model into the latent components of information processing leading up to choice selection and specifically probed BOLD activity encoding sequential temporal integration of decision evidence. Bounded evidence accumulation (or integration) constitutes a general framework to investigate how the brain processes decision evidence and ultimately determines choice behaviour (Forstmann et al., 2016; Ratcliff & McKoon, 2008; Ratcliff, Smith, & McKoon, 2015). It denotes the sequential sampling of noisy (perceptual or value-based) information about a stimulus (or set of stimuli) to some threshold level (that is, boundary) whence a choice is made (Forstmann et al., 2016; Shadlen & Kiani, 2013). Crucially, the efficiency of evidence accumulation is represented by the rate (or speed) at which evidence is accrued, that depends on the strength (or discriminability) of observed stimuli and is usually parameterised by the drift rate. In this study we set the

(dynamic) drift rate to the expected value difference of two available choice options to account for inter-trial variability in perceived choice difficulty (or discriminability). Other factors influencing the efficiency of evidence accumulation are decision noise and urgency (Bogacz et al., 2006). While the former describes the inherent stochasticity of the evidence sampling process that corrupts stimulus strength, the latter denotes the "urgency" to accelerate evidence accumulation to the decision bounds. Thus, the smaller the magnitude of the decision noise and/or urgency the smaller the rate of evidence accumulation and vice versa.

Most importantly, the framework of bounded evidence accumulation is robustly grounded in neurobiology (Gold & Shadlen, 2007; Shadlen & Kiani, 2013). Since the initial key finding that, during a motion discrimination task, the average firing rates recorded from single neurons in the lateral intraparietal cortex of two rhesus monkeys approximated accumulation-to-bound dynamics (Shadlen & Newsome, 2001), a plethora of independent studies have reported neural signatures of bounded evidence accumulation in the prefrontal and sensorimotor areas of human subjects using electroencephalography (EEG) (Kelly & O'Connell, 2013; Philiastides, Heekeren, & Sajda, 2014; Philiastides, Ratcliff, & Sajda, 2006; Wyart, de Gardelle, Scholl, & Summerfield, 2012), fMRI (Filimon, Philiastides, Nelson, Kloosterman, & Heekeren, 2013; Heekeren, Marrett, Bandettini, & Ungerleider, 2004; Ploran et al., 2007) and brain stimulation (Philiastides, Auksztulewicz, Heekeren, & Blankenburg, 2011). Notably, employing simultaneous EEG-fMRI a recent study identified neural correlates of bounded evidence accumulation in the medial PFC in the context of value-based decisions (Arabadzhiyska et al., 2022; Pisauro et al., 2017), thus lending further (neuroimaging) support to the proposal that bounded evidence accumulation is a domain-general decision mechanism (Krajbich et al., 2010).

Previous human fMRI studies have characterised the dmPFC as an accumulator region that acts as a decision value comparator and modulates motor cortex activity to implement choice (Hare, Schultz, Camerer, O'Doherty, & Rangel, 2011; Pedersen, Endestad, & Biele, 2015; Wunderlich, Rangel, & O'Doherty, 2009). Moreover, the dmPFC has been implicated in cost-benefit evaluation and is thought to determine willingness to engage in rewarded mental effort (Vassena, Deraeve, & Alexander, 2017). Cognitive effort is exerted through increasing commitment of cognitive control to improve behavioural performance, the benefits (that is, reward) of which are weighed against the costs of growing cognitive demands (Shenhav et al., 2017). A recent finding that stimulation of the dmPFC using transcranial alternating current stimulation increased cognitive effort expenditure for rewards, provided a causal link between dmPFC and effort-based choices (Soutschek, Nadporozhskaia, & Christian, 2022). Converging evidence that the dmPFC plays a key role in regulating effortful control is consistent with our interpretation that inflammation-induced attenuation of dmPFC BOLD activity supporting short evidence integration time serves the purpose of energy preservation by shifting neuronal resources away from relatively less costly neural tasks.

The experimental framework of effort-based decision making has been crucial in helping dissociate different components of reward processing that underlie inflammation-induced motivational impairments (Draper et al., 2018; Treadway, Buckholtz, Schwartzman,

Lambert, & Zald, 2009). Within this framework motivation is operationalised as willingness to expend (physical or mental) effort to obtain rewards as a function of reward magnitude and likelihood (Husain & Roiser, 2018). In line with the contention that inflammation primarily impairs effort-based decisions, animal studies have consistently documented that while inflammation spares reward sensitivity (or "liking"), it reduces effort expenditure (or reward "wanting") (Nunes et al., 2014; Vichaya, Hunt, & Dantzer, 2014; Yohn et al., 2016). Using a high effort/high reward versus low effort/low reward behavioural paradigm, one of these studies showed that the administration of lipopolysaccharide (LPS), a bacterial endotoxin used to elicit a systemic inflammatory response, shifted mice choice preference from the low effort/low reward towards the high effort/high reward option, therefore suggesting that effort investment is re-prioritised as a function of reward magnitude (Vichaya et al., 2014). An analogous behavioural finding was reported in humans (Lasselin et al., 2017). While in our experimental paradigm we did not modulate reward magnitude nor its likelihood, our results are consistent with the view that inflammation reallocates metabolic resources towards tasks that are (subjectively) deemed worth the effort in the face of increasing (internal and/or external) demands (Lasselin, 2021).

Dopamine signalling is believed to guide effort expenditure and allocation in pursuit of rewarding outcomes (Salamone, Correa, Ferrigno, et al., 2018; Salamone, Correa, Yang, et al., 2018; Walton & Bouret, 2019). A recently proposed unifying account of the role of dopamine in cost-benefit trade-offs posits that while increased stimulation of D_1 and D_2 dopamine receptors reduces effort costs, diminished stimulation of D_2 receptors reduces delay and risk costs (Soutschek, Jetter, & Tobler, 2023). Inflammation alters dopamine metabolism (Treadway et al., 2019). It decreases its synthesis via depletion of tetrahydrobiopterin (BH4) (Felger et al., 2013), an enzyme co-factor that is necessary for conversion of dopamine precursors into dopamine, and increases its reuptake by increasing the maximum rate of the dopamine transporter (Moron et al., 2003). The net effect of inflammation is thus to reduce dopamine bioavailabity, which is consistent with our (and previous) observation that inflammation diminishes activity in regions of the brain known to be major recipients of dopaminergic input and that have been implicated in effort-based decision making.

We replicated previous findings that experimentally induced mild inflammation lessens neural representation of the RPE in the striatum (Harrison et al., 2016; Treadway et al., 2017). It is possible that diminished neural encoding of value expectations associated with blunted RPE signalling disrupts integration of decision evidence at the time of choice.

Prior studies showed that increased levels of circulating pro-inflammatory cytokines (i.e. IL-6) induced using typhoid vaccination (Harrison et al., 2016) or a laboratory stress paradigm (Treadway et al., 2017) disrupted RPE signalling during a probabilistic RL task. Contrary to the behavioural paradigm employed in these studies, we did not have a neutral outcome nor separate appetitive (win versus neutral) and aversive (lose versus neutral) stimuli-outcome pairings in our task. We thus conclude that the finding of inflammation induced attenuation of RPE signals is robust to variations in reward learning paradigms. Blunted

striatal RPE signalling has already been linked to the severity of anhedonic symptoms in depression (Gradin et al., 2011; Kumar et al., 2008) and acute stress (Carvalheiro, Conceicao, Mesquita, & Seara-Cardoso, 2021). Moreover, we found RPE related activity in the putamen and amygdala to reliably classify response to self-help CBT in unmedicated depressed patients (Queirazza et al., 2019). Unlike RPE signals, Harrison et al. reported that punishment prediction errors (that is, BOLD activity negatively covarying with prediction error estimates in the aversive condition only) in the left insula were enhanced in response to inflammation. Consistent with the fMRI results they found that, behaviourally, inflammation increased punishment versus reward sensitivity (Harrison et al., 2016). Notably, in a subsequent study they showed that the tetracycline antibiotic minocycline attenuated the LPS-induced shift in punishment versus reward sensitivity, thus implicating microglial activation as putative molecular mechanism of the motivational impairments linked to inflammation (De Marco et al., 2023).

While the lack of significant behavioural and computational effects of inflammation in our study may be due to the insufficient power associated with our relatively small sample size and/or lower signal to noise ratio of the typhoid vaccination compared to other paradigms of controlled immune activation in humans such as LPS (Lasselin, Lekander, Benson, Schedlowski, & Engler, 2021), we showed that fMRI provided additional explanatory power to reveal subtle but significant effects of inflammation on the efficiency of decision dynamics in the brain.

An important limitation of our study is that the lack of females in our sample limits generalisation of our results to both sexes. It is also important to acknowledge that it is still not clear the extent to which the motivational changes associated with experimentally induced acute inflammation match those observed in depression and other mental disorders. Likewise, while the typhoid vaccine model of acute and transient inflammation circumvents the confounding influence of prolonged stress and pain associated with chronic inflammation, further work is necessary to elucidate the neural pathways and computational mechanisms associated with long-term inflammation.

5. Conclusion

In this study we explicitly modelled the neural mechanisms underpinning integration of decision evidence, which converging empirical evidence has validated as a key processing stage of decision making. To the best of our knowledge, this is the first study to show that mild, experimentally induced inflammation alters neural activity supporting bounded evidence accumulation at the time of choice. The importance of elucidating the effects of inflammation on the neural implementation of decision dynamics to better unpack its links with psychopathology is underscored by converging behavioural findings that bounded accumulation of decision evidence is impaired in depression (Cataldo, Scheuer, Maksimovskiy, Germine, & Dillon, 2023; Lawlor et al., 2020) and other mental disorders (Banca et al., 2015; Heathcote et al., 2015; Karalunas, Huang-Pollock, & Nigg, 2012; Sripada & Weigard, 2021). Behavioural and neural signatures of the efficiency of bounded evidence accumulation thus represent a domain-general transdiagnostic risk factor for psychopathology (Weigard & Sripada, 2021).

Declaration of Competing Interest

The authors declare that they have no known competing financial interests or personal relationships that could have appeared to influence the work reported in this paper.

Data availability

Data and code will be made available upon request.

Acknowledgements

The study was funded by a clinical lecturer starter grant awarded to R.K. by the Academy of Medical Sciences. F.Q. was supported by the JMAS Sim Fellowship awarded by the Royal College of Physician of Edinburgh. M.G.P. was supported by a European Research Council grant (ERC, DyNeRfusion, 865003).

References

Arabadzhiyska, D. H., Garrod, O. G. B., Fouragnan, E., De Luca, E., Schyns, P. G., & Philiastides, M. G. (2022). A Common Neural Account for Social and Nonsocial Decisions. *J Neurosci, 42*(48), 9030-9044.

Balsdon, T., Verdonck, S., Loossens, T., & Philiastides, M. G. (2023). Secondary motor integration as a final arbiter in sensorimotor decision-making. *PLoS Biol, 21*(7), e3002200.

Banca, P., Vestergaard, M. D., Rankov, V., Baek, K., Mitchell, S., Lapa, T., et al. (2015). Evidence accumulation in obsessive-compulsive disorder: the role of uncertainty and monetary reward on perceptual decision-making thresholds. *Neuropsychopharmacology, 40*(5), 1192-1202.

Barr, D. J., Levy, R., Scheepers, C., & Tily, H. J. (2013). Random effects structure for confirmatory hypothesis testing: Keep it maximal. *J Mem Lang, 68*(3).

Beck, A. T., Steer, R. A., & Brown, G. (1996). Beck Depression Inventory-II (BDI-II).

Bertone-Johnson, E. R., Ronnenberg, A. G., Houghton, S. C., Nobles, C., Zagarins, S. E., Takashima-Uebelhoer, B. B., et al. (2014). Association of inflammation markers with menstrual symptom severity and premenstrual syndrome in young women. *Hum Reprod, 29*(9), 1987-1994.

Blum, C. A., Muller, B., Huber, P., Kraenzlin, M., Schindler, C., De Geyter, C., et al. (2005). Low-grade inflammation and estimates of insulin resistance during the menstrual cycle in lean and overweight women. *J Clin Endocrinol Metab, 90*(6), 3230-3235.

Bogacz, R. (2007). Optimal decision-making theories: linking neurobiology with behaviour. *Trends Cogn Sci, 11*(3), 118-125.

Bogacz, R., Brown, E., Moehlis, J., Holmes, P., & Cohen, J. D. (2006). The physics of optimal decision making: a formal analysis of models of performance in two-alternative forced-choice tasks. *Psychol Rev, 113*(4), 700-765.

Boyle, C. C., Kuhlman, K. R., Dooley, L. N., Haydon, M. D., Robles, T. F., Ang, Y. S., et al. (2019). Inflammation and dimensions of reward processing following exposure to the influenza vaccine. *Psychoneuroendocrinology, 102*, 16-23.

Boyle, C. C., Stanton, A. L., Eisenberger, N. I., Seeman, T. E., & Bower, J. E. (2020). Effects of stress-induced inflammation on reward processing in healthy young women. *Brain Behav Immun, 83*, 126-134.

Brydon, L., Walker, C., Wawrzyniak, A., Whitehead, D., Okamura, H., Yajima, J., et al. (2009). Synergistic effects of psychological and immune stressors on inflammatory cytokine and sickness responses in humans. *Brain Behav Immun, 23*(2), 217-224.

884 Burrows, K., Stewart, J. L., Kuplicki, R., Figueroa-Hall, L., Spechler, P. A., Zheng, H., et al.
885 (2021). Elevated peripheral inflammation is associated with attenuated striatal
886 reward anticipation in major depressive disorder. *Brain Behav Immun, 93*, 214-225.

887 Capuron, L., Pagnoni, G., Drake, D. F., Woolwine, B. J., Spivey, J. R., Crowe, R. J., et al. (2012).
888 Dopaminergic mechanisms of reduced basal ganglia responses to hedonic reward
889 during interferon alfa administration. *Arch Gen Psychiatry, 69*(10), 1044-1053.

890 Carvalheiro, J., Conceicao, V. A., Mesquita, A., & Seara-Cardoso, A. (2021). Acute stress
891 blunts prediction error signals in the dorsal striatum during reinforcement learning.
892 *Neurobiol Stress, 15*, 100412.

893 Cataldo, A. M., Scheuer, L., Maksimovskiy, A. L., Germine, L. T., & Dillon, D. G. (2023).
894 Abnormal evidence accumulation underlies the positive memory deficit in
895 depression. *J Exp Psychol Gen, 152*(1), 139-156.

896 Challis, J. R., Lockwood, C. J., Myatt, L., Norman, J. E., Strauss, J. F., 3rd, & Petraglia, F.
897 (2009). Inflammation and pregnancy. *Reprod Sci, 16*(2), 206-215.

898 Dantzer, R. (2001). Cytokine-induced sickness behavior: where do we stand? *Brain Behav*
899 *Immun, 15*(1), 7-24.

900 Dantzer, R., & Kelley, K. W. (2007). Twenty years of research on cytokine-induced sickness
901 behavior. *Brain Behav Immun, 21*(2), 153-160.

902 Dantzer, R., O'Connor, J. C., Freund, G. G., Johnson, R. W., & Kelley, K. W. (2008). From
903 inflammation to sickness and depression: when the immune system subjugates the
904 brain. *Nat Rev Neurosci, 9*(1), 46-56.

905 De Marco, R., Barritt, A. W., Cercignani, M., Cabbai, G., Colasanti, A., & Harrison, N. A.
906 (2023). Inflammation-induced reorientation of reward versus punishment sensitivity
907 is attenuated by minocycline. *Brain Behav Immun, 111*, 320-327.

908 Divani, A. A., Luo, X., Datta, Y. H., Flaherty, J. D., & Panoskaltsis-Mortari, A. (2015). Effect of
909 oral and vaginal hormonal contraceptives on inflammatory blood biomarkers.
910 *Mediators Inflamm, 2015*, 379501.

911 Draper, A., Koch, R. M., van der Meer, J. W., Aj Apps, M., Pickkers, P., Husain, M., et al.
912 (2018). Effort but not Reward Sensitivity is Altered by Acute Sickness Induced by
913 Experimental Endotoxemia in Humans. *Neuropsychopharmacology, 43*(5), 1107-
914 1118.

915 Eisenberger, N. I., Berkman, E. T., Inagaki, T. K., Rameson, L. T., Mashal, N. M., & Irwin, M. R.
916 (2010). Inflammation-induced anhedonia: endotoxin reduces ventral striatum
917 responses to reward. *Biol Psychiatry, 68*(8), 748-754.

918 Felger, J. C., Li, L., Marvar, P. J., Woolwine, B. J., Harrison, D. G., Raison, C. L., et al. (2013).
919 Tyrosine metabolism during interferon-alpha administration: association with fatigue
920 and CSF dopamine concentrations. *Brain Behav Immun, 31*, 153-160.

Felger, J. C., Li, Z., Haroon, E., Woolwine, B. J., Jung, M. Y., Hu, X., et al. (2016). Inflammation is associated with decreased functional connectivity within corticostriatal reward circuitry in depression. *Mol Psychiatry, 21*(10), 1358-1365.

Filimon, F., Philiastides, M. G., Nelson, J. D., Kloosterman, N. A., & Heekeren, H. R. (2013). How embodied is perceptual decision making? Evidence for separate processing of perceptual and motor decisions. *J Neurosci, 33*(5), 2121-2136.

Forstmann, B. U., Ratcliff, R., & Wagenmakers, E. J. (2016). Sequential Sampling Models in Cognitive Neuroscience: Advantages, Applications, and Extensions. *Annu Rev Psychol, 67*, 641-666.

Fouragnan, E., Queirazza, F., Retzler, C., Mullinger, K. J., & Philiastides, M. G. (2017). Spatiotemporal neural characterization of prediction error valence and surprise during reward learning in humans. *Sci Rep, 7*(1), 4762.

Fouragnan, E., Retzler, C., Mullinger, K., & Philiastides, M. G. (2015). Two spatiotemporally distinct value systems shape reward-based learning in the human brain. *Nat Commun, 6*, 8107.

Franzen, L., Delis, I., De Sousa, G., Kayser, C., & Philiastides, M. G. (2020). Auditory information enhances post-sensory visual evidence during rapid multisensory decision-making. *Nat Commun, 11*(1), 5440.

Gherman, S., Markowitz, N., Tostaeva, G., Espinal, E., Mehta, A. D., O'Connell, R. G., et al. (2024). Intracranial electroencephalography reveals effector-independent evidence accumulation dynamics in multiple human brain regions. *Nat Hum Behav*.

Gherman, S., & Philiastides, M. G. (2015). Neural representations of confidence emerge from the process of decision formation during perceptual choices. *Neuroimage, 106*, 134-143.

Gold, J. I., & Shadlen, M. N. (2007). The neural basis of decision making. *Annu Rev Neurosci, 30*, 535-574.

Gradin, V. B., Kumar, P., Waiter, G., Ahearn, T., Stickle, C., Milders, M., et al. (2011). Expected value and prediction error abnormalities in depression and schizophrenia. *Brain, 134*(Pt 6), 1751-1764.

Hare, T. A., Schultz, W., Camerer, C. F., O'Doherty, J. P., & Rangel, A. (2011). Transformation of stimulus value signals into motor commands during simple choice. *Proc Natl Acad Sci U S A, 108*(44), 18120-18125.

Harrison, N. A., Brydon, L., Walker, C., Gray, M. A., Steptoe, A., & Critchley, H. D. (2009). Inflammation causes mood changes through alterations in subgenual cingulate activity and mesolimbic connectivity. *Biol Psychiatry, 66*(5), 407-414.

Harrison, N. A., Voon, V., Cercignani, M., Cooper, E. A., Pessiglione, M., & Critchley, H. D. (2016). A Neurocomputational Account of How Inflammation Enhances Sensitivity to Punishments Versus Rewards. *Biol Psychiatry, 80*(1), 73-81.

Hart, B. L. (1988). Biological basis of the behavior of sick animals. *Neurosci Biobehav Rev, 12*(2), 123-137.

Heathcote, A., Suraev, A., Curley, S., Gong, Q., Love, J., & Michie, P. T. (2015). Decision processes and the slowing of simple choices in schizophrenia. *J Abnorm Psychol, 124*(4), 961-974.

Hedberg, E. C., & Ayers, S. (2015). The power of a paired t-test with a covariate. *Soc Sci Res, 50*, 277-291.

Heekeren, H. R., Marrett, S., Bandettini, P. A., & Ungerleider, L. G. (2004). A general mechanism for perceptual decision-making in the human brain. *Nature, 431*(7010), 859-862.

Husain, M., & Roiser, J. P. (2018). Neuroscience of apathy and anhedonia: a transdiagnostic approach. *Nat Rev Neurosci, 19*(8), 470-484.

Karalunas, S. L., Huang-Pollock, C. L., & Nigg, J. T. (2012). Decomposing attention-deficit/hyperactivity disorder (ADHD)-related effects in response speed and variability. *Neuropsychology, 26*(6), 684-694.

Kelly, S. P., & O'Connell, R. G. (2013). Internal and external influences on the rate of sensory evidence accumulation in the human brain. *J Neurosci, 33*(50), 19434-19441.

Krajbich, I., Armel, C., & Rangel, A. (2010). Visual fixations and the computation and comparison of value in simple choice. *Nat Neurosci, 13*(10), 1292-1298.

Krishnadas, R., & Cavanagh, J. (2012). Depression: an inflammatory illness? *J Neurol Neurosurg Psychiatry, 83*(5), 495-502.

Kumar, P., Waiter, G., Ahearn, T., Milders, M., Reid, I., & Steele, J. D. (2008). Abnormal temporal difference reward-learning signals in major depression. *Brain, 131*(Pt 8), 2084-2093.

Lasselin, J. (2021). Back to the future of psychoneuroimmunology: Studying inflammation-induced sickness behavior. *Brain Behav Immun Health, 18*, 100379.

Lasselin, J., Lekander, M., Benson, S., Schedlowski, M., & Engler, H. (2021). Sick for science: experimental endotoxemia as a translational tool to develop and test new therapies for inflammation-associated depression. *Mol Psychiatry, 26*(8), 3672-3683.

Lasselin, J., Treadway, M. T., Lacourt, T. E., Soop, A., Olsson, M. J., Karshikoff, B., et al. (2017). Lipopolysaccharide Alters Motivated Behavior in a Monetary Reward Task: a Randomized Trial. *Neuropsychopharmacology, 42*(4), 801-810.

991 Lawlor, V. M., Webb, C. A., Wiecki, T. V., Frank, M. J., Trivedi, M., Pizzagalli, D. A., et al.
992 (2020). Dissecting the impact of depression on decision-making. *Psychol Med,*
993 *50*(10), 1613-1622.

994 Luzardo, A., Alonso, E., & Mondragon, E. (2017). A Rescorla-Wagner drift-diffusion model of
995 conditioning and timing. *PLoS Comput Biol, 13*(11), e1005796.

996 McNair, D. M., Lorr, M., & Droppleman, L. F. (1971). Manual for the Profile of Mood States.
997 *San Diego, CA: Educational and Industrial Testing Service*.

998 Michopoulos, V., Powers, A., Gillespie, C. F., Ressler, K. J., & Jovanovic, T. (2017).
999 Inflammation in Fear- and Anxiety-Based Disorders: PTSD, GAD, and Beyond.
1000 *Neuropsychopharmacology, 42*(1), 254-270.

1001 Miller, A. H. (2020). Beyond depression: the expanding role of inflammation in psychiatric
1002 disorders. *World Psychiatry, 19*(1), 108-109.

1003 Miller, A. H., Maletic, V., & Raison, C. L. (2009). Inflammation and its discontents: the role of
1004 cytokines in the pathophysiology of major depression. *Biol Psychiatry, 65*(9), 732-
1005 741.

1006 Miller, A. H., & Raison, C. L. (2016). The role of inflammation in depression: from
1007 evolutionary imperative to modern treatment target. *Nat Rev Immunol, 16*(1), 22-34.

1008 Moieni, M., Muscatell, K. A., Jevtic, I., Breen, E. C., Irwin, M. R., & Eisenberger, N. I. (2019).
1009 Sex Differences in the Effect of Inflammation on Subjective Social Status: A
1010 Randomized Controlled Trial of Endotoxin in Healthy Young Adults. *Front Psychol, 10*,
1011 2167.

1012 Moron, J. A., Zakharova, I., Ferrer, J. V., Merrill, G. A., Hope, B., Lafer, E. M., et al. (2003).
1013 Mitogen-activated protein kinase regulates dopamine transporter surface expression
1014 and dopamine transport capacity. *J Neurosci, 23*(24), 8480-8488.

1015 Nunes, E. J., Randall, P. A., Estrada, A., Epling, B., Hart, E. E., Lee, C. A., et al. (2014). Effort-
1016 related motivational effects of the pro-inflammatory cytokine interleukin 1-beta:
1017 studies with the concurrent fixed ratio 5/ chow feeding choice task.
1018 *Psychopharmacology (Berl), 231*(4), 727-736.

1019 O'Doherty, J. P., Hampton, A., & Kim, H. (2007). Model-based fMRI and its application to
1020 reward learning and decision making. *Ann N Y Acad Sci, 1104*, 35-53.

1021 Palm, M., Axelsson, O., Wernroth, L., Larsson, A., & Basu, S. (2013). Involvement of
1022 inflammation in normal pregnancy. *Acta Obstet Gynecol Scand, 92*(5), 601-605.

1023 Palminteri, S., Wyart, V., & Koechlin, E. (2017). The Importance of Falsification in
1024 Computational Cognitive Modeling. *Trends Cogn Sci, 21*(6), 425-433.

Pedersen, M. L., Endestad, T., & Biele, G. (2015). Evidence Accumulation and Choice Maintenance Are Dissociated in Human Perceptual Decision Making. *PLoS One, 10*(10), e0140361.

Pedersen, M. L., Frank, M. J., & Biele, G. (2017). The drift diffusion model as the choice rule in reinforcement learning. *Psychon Bull Rev, 24*(4), 1234-1251.

Pernet, C. R., Wilcox, R., & Rousselet, G. A. (2012). Robust correlation analyses: false positive and power validation using a new open source matlab toolbox. *Front Psychol, 3*, 606.

Philiastides, M. G., Auksztulewicz, R., Heekeren, H. R., & Blankenburg, F. (2011). Causal role of dorsolateral prefrontal cortex in human perceptual decision making. *Curr Biol, 21*(11), 980-983.

Philiastides, M. G., Heekeren, H. R., & Sajda, P. (2014). Human scalp potentials reflect a mixture of decision-related signals during perceptual choices. *J Neurosci, 34*(50), 16877-16889.

Philiastides, M. G., Ratcliff, R., & Sajda, P. (2006). Neural representation of task difficulty and decision making during perceptual categorization: a timing diagram. *J Neurosci, 26*(35), 8965-8975.

Pisauro, M. A., Fouragnan, E., Retzler, C., & Philiastides, M. G. (2017). Neural correlates of evidence accumulation during value-based decisions revealed via simultaneous EEG-fMRI. *Nat Commun, 8*, 15808.

Pizzagalli, D. A., Jahn, A. L., & O'Shea, J. P. (2005). Toward an objective characterization of an anhedonic phenotype: a signal-detection approach. *Biol Psychiatry, 57*(4), 319-327.

Ploran, E. J., Nelson, S. M., Velanova, K., Donaldson, D. I., Petersen, S. E., & Wheeler, M. E. (2007). Evidence accumulation and the moment of recognition: dissociating perceptual recognition processes using fMRI. *J Neurosci, 27*(44), 11912-11924.

Polania, R., Krajbich, I., Grueschow, M., & Ruff, C. C. (2014). Neural oscillations and synchronization differentially support evidence accumulation in perceptual and value-based decision making. *Neuron, 82*(3), 709-720.

Queirazza, F., Fouragnan, E., Steele, J. D., Cavanagh, J., & Philiastides, M. G. (2019). Neural correlates of weighted reward prediction error during reinforcement learning classify response to cognitive behavioral therapy in depression. *Sci Adv, 5*(7), eaav4962.

Ratcliff, R., & McKoon, G. (2008). The diffusion decision model: theory and data for two-choice decision tasks. *Neural Comput, 20*(4), 873-922.

Ratcliff, R., Smith, P. L., & McKoon, G. (2015). Modeling Regularities in Response Time and Accuracy Data with the Diffusion Model. *Curr Dir Psychol Sci, 24*(6), 458-470.

Sacks, G. P., Studena, K., Sargent, K., & Redman, C. W. (1998). Normal pregnancy and preeclampsia both produce inflammatory changes in peripheral blood leukocytes akin to those of sepsis. *Am J Obstet Gynecol, 179*(1), 80-86.

Said, E. A., Al-Reesi, I., Al-Shizawi, N., Jaju, S., Al-Balushi, M. S., Koh, C. Y., et al. (2021). Defining IL-6 levels in healthy individuals: A meta-analysis. *J Med Virol, 93*(6), 3915-3924.

Salamone, J. D., Correa, M., Ferrigno, S., Yang, J. H., Rotolo, R. A., & Presby, R. E. (2018). The Psychopharmacology of Effort-Related Decision Making: Dopamine, Adenosine, and Insights into the Neurochemistry of Motivation. *Pharmacol Rev, 70*(4), 747-762.

Salamone, J. D., Correa, M., Yang, J. H., Rotolo, R., & Presby, R. (2018). Dopamine, Effort-Based Choice, and Behavioral Economics: Basic and Translational Research. *Front Behav Neurosci, 12*, 52.

Schultz, W., Dayan, P., & Montague, P. R. (1997). A neural substrate of prediction and reward. *Science, 275*(5306), 1593-1599.

Shadlen, M. N., & Kiani, R. (2013). Decision making as a window on cognition. *Neuron, 80*(3), 791-806.

Shadlen, M. N., & Newsome, W. T. (2001). Neural basis of a perceptual decision in the parietal cortex (area LIP) of the rhesus monkey. *J Neurophysiol, 86*(4), 1916-1936.

Shenhav, A., Musslick, S., Lieder, F., Kool, W., Griffiths, T. L., Cohen, J. D., et al. (2017). Toward a Rational and Mechanistic Account of Mental Effort. *Annu Rev Neurosci, 40*, 99-124.

Soutschek, A., Jetter, A., & Tobler, P. N. (2023). Toward a Unifying Account of Dopamine's Role in Cost-Benefit Decision Making. *Biol Psychiatry Glob Open Sci, 3*(2), 179-186.

Soutschek, A., Nadporozhskaia, L., & Christian, P. (2022). Brain stimulation over dorsomedial prefrontal cortex modulates effort-based decision making. *Cogn Affect Behav Neurosci, 22*(6), 1264-1274.

Spielberger, C. D. (1983). State-Trait Anxiety Inventory for Adults (STAI-AD).

Sripada, C., & Weigard, A. (2021). Impaired Evidence Accumulation as a Transdiagnostic Vulnerability Factor in Psychopathology. *Front Psychiatry, 12*, 627179.

Stefanov, K., McLean, J., Allan, B., Cavanagh, J., & Krishnadas, R. (2020). Mild inflammation causes a reduction in resting-state amplitude of low-frequency fluctuation in healthy adult males. *Brain Neurosci Adv, 4*, 2398212820949353.

Stefanov, K., McLean, J., McColl, A., Basu, N., Cavanagh, J., & Krishnadas, R. (2020). Mild Inflammation in Healthy Males Induces Fatigue Mediated by Changes in Effective Connectivity Within the Insula. *Biol Psychiatry Cogn Neurosci Neuroimaging, 5*(9), 865-874.

Strike, P. C., Wardle, J., & Steptoe, A. (2004). Mild acute inflammatory stimulation induces transient negative mood. *J Psychosom Res, 57*(2), 189-194.

Treadway, M. T., Admon, R., Arulpragasam, A. R., Mehta, M., Douglas, S., Vitaliano, G., et al. (2017). Association Between Interleukin-6 and Striatal Prediction-Error Signals Following Acute Stress in Healthy Female Participants. *Biol Psychiatry, 82*(8), 570-577.

Treadway, M. T., Bossaller, N. A., Shelton, R. C., & Zald, D. H. (2012). Effort-based decision-making in major depressive disorder: a translational model of motivational anhedonia. *J Abnorm Psychol, 121*(3), 553-558.

Treadway, M. T., Buckholtz, J. W., Schwartzman, A. N., Lambert, W. E., & Zald, D. H. (2009). Worth the 'EEfRT'? The effort expenditure for rewards task as an objective measure of motivation and anhedonia. *PLoS One, 4*(8), e6598.

Treadway, M. T., Cooper, J. A., & Miller, A. H. (2019). Can't or Won't? Immunometabolic Constraints on Dopaminergic Drive. *Trends Cogn Sci, 23*(5), 435-448.

Vassena, E., Deraeve, J., & Alexander, W. H. (2017). Predicting Motivation: Computational Models of PFC Can Explain Neural Coding of Motivation and Effort-based Decision-making in Health and Disease. *J Cogn Neurosci, 29*(10), 1633-1645.

Verdonck, S., Loossens, T., & Philiastides, M. G. (2021). The Leaky Integrating Threshold and its impact on evidence accumulation models of choice response time (RT). *Psychol Rev, 128*(2), 203-221.

Vichaya, E. G., Hunt, S. C., & Dantzer, R. (2014). Lipopolysaccharide reduces incentive motivation while boosting preference for high reward in mice. *Neuropsychopharmacology, 39*(12), 2884-2890.

Walton, M. E., & Bouret, S. (2019). What Is the Relationship between Dopamine and Effort? *Trends Neurosci, 42*(2), 79-91.

Webster, K., Cella, D., & Yost, K. (2003). The Functional Assessment of Chronic Illness Therapy (FACIT) Measurement System: properties, applications, and interpretation. *Health Qual Life Outcomes, 1*, 79.

Weigard, A., & Sripada, C. (2021). Task-general efficiency of evidence accumulation as a computationally-defined neurocognitive trait: Implications for clinical neuroscience. *Biol Psychiatry Glob Open Sci, 1*(1), 5-15.

Weiskopf, N., Hutton, C., Josephs, O., & Deichmann, R. (2006). Optimal EPI parameters for reduction of susceptibility-induced BOLD sensitivity losses: a whole-brain analysis at 3 T and 1.5 T. *Neuroimage, 33*(2), 493-504.

Wright, C. E., Strike, P. C., Brydon, L., & Steptoe, A. (2005). Acute inflammation and negative mood: mediation by cytokine activation. *Brain Behav Immun, 19*(4), 345-350.

Wunderlich, K., Rangel, A., & O'Doherty, J. P. (2009). Neural computations underlying action-based decision making in the human brain. *Proc Natl Acad Sci U S A, 106*(40), 17199-17204.

Wyart, V., de Gardelle, V., Scholl, J., & Summerfield, C. (2012). Rhythmic fluctuations in evidence accumulation during decision making in the human brain. *Neuron, 76*(4), 847-858.

Yohn, S. E., Arif, Y., Haley, A., Tripodi, G., Baqi, Y., Muller, C. E., et al. (2016). Effort-related motivational effects of the pro-inflammatory cytokine interleukin-6: pharmacological and neurochemical characterization. *Psychopharmacology (Berl), 233*(19-20), 3575-3586.

Highlights

- We investigated the effects of typhoid vaccination on neural activity supporting decision making and reward learning during a behavioural task using model-based functional resonance imaging and a randomised, placebo-controlled, crossover design.
- Typhoid vaccination decreased haemodynamic activity in the dorsomedial prefrontal cortex indexing efficiency of decision dynamics as a function of integration time.
- Typhoid vaccination attenuated reward prediction error signalling in the ventral striatum and amygdala.